

## pH-Responsive Quantum Dots via an Albumin Polymer Surface Coating

Yuzhou Wu,<sup>†</sup> Sabyasachi Chakraborty,<sup>†</sup> Radu A. Gropeanu,<sup>‡</sup> Joerg Wilhelmi,<sup>‡</sup> Yang Xu,<sup>†</sup>  
Kai Shih Er,<sup>†</sup> Seah Ling Kuan,<sup>†</sup> Kaloian Koynov,<sup>‡</sup> Yinthai Chan,<sup>\*,†,§</sup> and Tanja Weil<sup>\*,†,‡</sup>

Department of Chemistry, National University of Singapore, 3 Science Drive 3, Singapore 117543, Max Planck Institute for Polymer Research, Ackermannweg 10, D-55128 Mainz, Germany, and Institute of Research and Engineering, A\*STAR, Singapore 117602

Received November 18, 2009; E-mail: chmchany@nus.edu.sg; chmweilt@nus.edu.sg

Quantum dots (QDs) have many unique features, such as high resistance to photobleaching and a wide excitation range, which make them promising as fluorophores for biomedical diagnostic applications.<sup>1</sup> Conventional as-synthesized QDs are hydrophobic. Facilitating their long-term, aggregation-free use in an aqueous environment via surface coating with suitable hydrophilic substituents represents a key challenge.<sup>2</sup> It was previously reported that ligands with more than one anchor group interacting with the QD surface (i.e., polydentate ligands) showed improved stability and reduced ligand loss<sup>3–5</sup> and that capping groups such as dihydroliipoic acid (DHLLA) were determined to be particularly effective.<sup>5–9</sup> Following this motif, we have synthesized a novel peptide–polymer hybrid material consisting of a biocompatible peptide backbone of defined chain length having poly(ethylene oxide) (PEO) side chains to reduce nonspecific interactions as well as a high number of thiol (originating from thioctic acid, TA) and amine anchor groups interacting with the QD surface. This peptide–polymer hybrid was derived from human serum albumin (HSA) utilizing reaction sequences that facilitated the stabilization of linear denatured human serum albumins (dHSAs) in aqueous solution. In contrast to dHSA, the linearized multifunctional albumin peptide–polymer hybrids described herein represent stable macromolecules that are particularly suitable as surface ligands for QDs, as they impart biocompatibility, high stability in an aqueous environment, and multiple functional groups facilitating further modifications for various applications. In comparison with other polymers, the peptide–polymer hybrids reported in this work benefit from a precisely known length of the main chain and a distinct number of functional groups at defined locations (e.g., 100 carboxylic acid groups of glutamate and aspartate side chains) that allow for further chemical modifications. We demonstrate that unlike previously reported fluorescence resonance energy transfer (FRET)-based QD pH-sensing schemes,<sup>10–12</sup> our peptide–polymer hybrid-coated ODs have a direct optical response to changes in pH. This work presents a facile route to biocompatible, multivalent surface coatings on QDs that may contribute to the development of QD-based pH sensors. QD-based pH sensors would potentially be able to give better fluorescence signals in comparison with conventional organic-based fluorescent pH sensors, especially in cases where it is necessary to use two-photon excitation for imaging and where continuous monitoring of the pH and therefore continuous excitation is required.

A schematic of the synthesis of dHSA–PEO–TA hybrids (**6**) as surface ligands for QDs is given in Figure 1. First, HSA (**1**) was dissolved in a urea/phosphate buffer (pH 7.4). The reducing agent tris(2-carboxyethyl)phosphine hydrochloride was then applied to reduce the 34 disulfide bridges within the tertiary structure of

HSA, giving dHSA (**2**). Michael addition of **2** with PEO-5000 carrying a single maleimide group yielded dHSA–PEO (**4**), which was very soluble in aqueous solution. *N*-(2-Aminoethyl)maleimide trifluoroacetate salt (**3**) was applied in order to react with the remaining thiol groups to improve the stability and shelf life of **4**. Subsequently, the condensation reaction between the free amino groups of the lysine side chains of **4** and thioctic acid groups activated via *N*-hydroxysuccinimide (NHS) ester **5** in dimethylformamide in the presence of NaHCO<sub>3</sub> resulted in the formation of multifunctional dHSA–PEO–TA hybrid **6**.

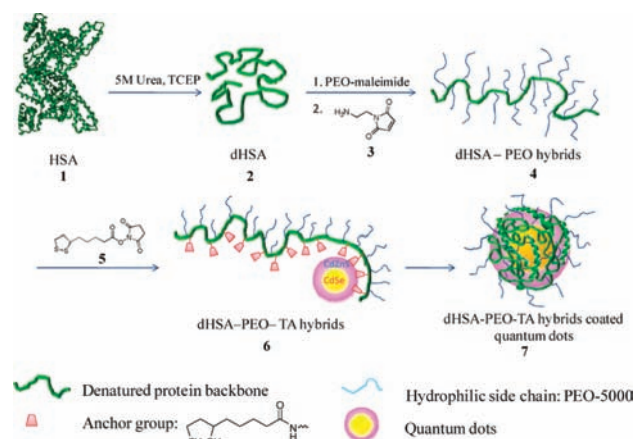


**Figure 1.** Synthesis of polypeptide hybrids **4** and **6** and an illustration of a QD coated with dHSA–PEO–TA hybrid. While it was possible for **6** and consequently **7** to include more than one QD, such occurrences were rare, and the majority of conjugates contained a single QD.

SDS–PAGE revealed a significantly increased molecular weight for **4** in the range 150–210 kDa after attachment of the PEO chains. An additional slight increase in the molecular weight was found after conjugation of the thioctic acid groups to **4** [Figure S3 in the Supporting Information (SI)]. Figure S7 shows a typical MALDI–TOF mass spectrum of **6** with an average molecular weight of ~200 kDa, which corresponds to the SDS–PAGE result (Figure S3). Furthermore, the polymer dispersity of **6** was investigated by gel-permeation chromatography (GPC). A sharp signal indicative of a narrow size distribution and low dispersity was detected (Figure S6). However, because of the unique architecture of **6**, no GPC standard with a similar structure and polarity could be identified, thus preventing size estimation via GPC. In this context, commonly used standards such as PEO of different chain lengths and Dextran were not applicable. In order to assess the number of TA groups in **6**, 4,4'-dithiodipyridine (DPS) was applied. This reagent is reduced in the presence of free thiol groups, forming 4-thiopyridone with a characteristic absorbance maximum at 325 nm (Scheme S1

<sup>†</sup> National University of Singapore.

<sup>‡</sup> Max Planck Institute for Polymer Research.

<sup>§</sup> A\*STAR.

and Figure S5). A good correlation between the TA concentration and the absorption of 4-thiopyridone was obtained, allowing a quantification of the free thiol groups of **6**.

Three different batches of **6** were investigated, and an average  $22 \pm 5$  TA groups (corresponding to  $\sim 44$  thiol groups) was very reproducibly obtained. In addition,  $\sim 40$  amino groups of lysine residues are also available to interact with the QD surface. Coupling of the dHSA–PEO–TA hybrids **6** to hydrophobic as-synthesized core–shell CdSe–CdZnS QDs proceeded via reduction of the disulfide group of the TA substituents in **6** with  $\text{NaBH}_4$  under argon to afford DHLA followed by addition of processed QDs dispersed in a minimum amount of tetrahydrofuran under vigorous stirring. The solution was stirred overnight, and the unreacted QDs were filtered out. The coated QDs were homogeneously dispersed in water (Figure S4). The emission spectrum of QDs coated with **6** revealed a slight bathochromic shift relative to the as-synthesized QDs in hexane, consistent with previous reports on ligand exchange with thioalkyl acids.<sup>13</sup> The quantum yield (QY) of the as-synthesized core–shell QDs decreased from  $\sim 48\%$  in hexane to  $\sim 16\%$  on average in water, which is typical of QD ligand-exchange processes.<sup>4,8</sup> Fluorescence correlation spectroscopy (FCS) measurements afforded a hydrodynamic diameter of  $\sim 34$  nm, consistent with the diameter of  $\sim 30$  nm obtained using dynamic light scattering (DLS) measurements (see the SI). The narrow hydrodynamic size dispersion from the DLS measurements suggested that a statistical distribution of QDs per polymer was unlikely, and transmission electron microscopy (TEM) of the QD–polymer conjugates revealed that the vast majority of conjugates contained a single QD (see Figure 4 and the SI). We found that the albumin peptide–polymer-coated QDs **7** were stable in water under ambient conditions for months with respect to aggregation (according to DLS) as well as QY.

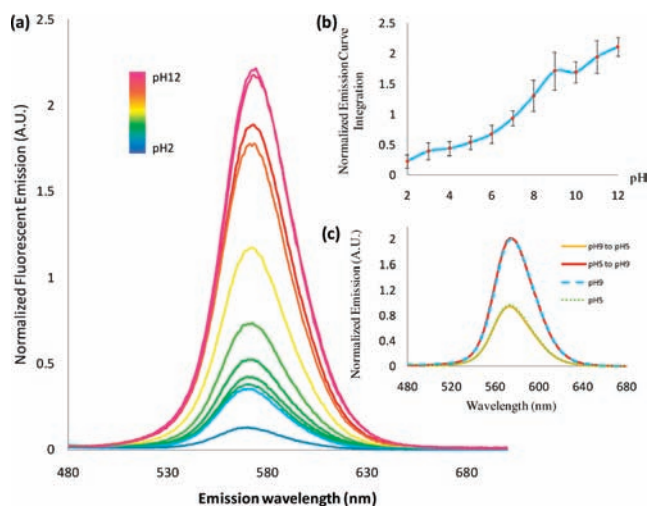


**Figure 2.** (a) Emission intensity of **7** at different pH ( $\lambda_{\text{exc}} = 254$  nm). (b) Integrated emission intensities vs pH based on four consecutive measurements. (c) Reversibility of the pH responsiveness between pH 5 and 9 based on three independent measurements. The emission intensity was recovered after increasing the pH from 5 to 9 as well as decreasing the pH from 9 to 5.

When the stability of **7** at different pH values was assessed, surprisingly strong optical responses to changes in pH were observed. A series of universal buffer solutions with pH ranging systematically from 3 to 12 were prepared as described in the SI, and the fluorescence intensities of mixtures of **7** in buffers of different pH were monitored with a fluorescence microplate reader.

Significant changes in emission intensity were observed as the pH was varied, as depicted in Figure 2a,b.

As the pH changed from 2 to 12, the QY of **7** increased nearly 10-fold (Table 1). Within the physiological pH range 5–9, where the most significant increases in QYs were found, we verified that these changes were fully reversible, as shown in Figure 2c. Additionally, no discernible shifts in the peak emission were observed at the different pH values. These findings collectively suggest that neither shell degradation<sup>14</sup> and hole trapping<sup>15</sup> from thiolate formation nor aggregation through irreversible ligand loss could explain the changes in QY.

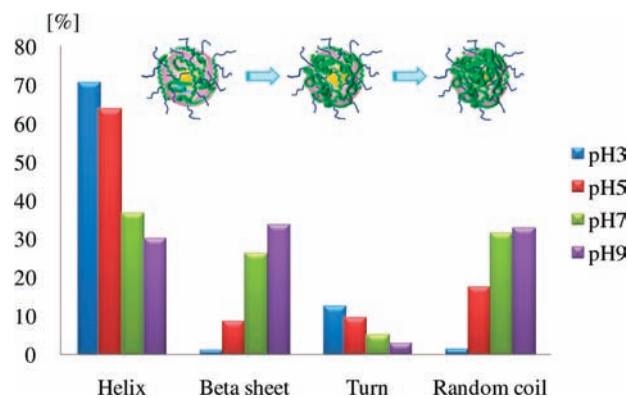


**Figure 3.** Changes in the secondary structure of **6** at different pH values.

The changes in the PL efficiency at different pH may broadly be attributed to corresponding changes in surface passivation of the QD. We hypothesized that structural changes in the dHSA–PEO–TA hybrids **6** at different pH may influence their ability to interact with the QD surface. In order to verify this assertion, the secondary structure of **6** was investigated via circular dichroism (CD) at different pH values, as summarized in Figure 3 and Table 1. At acidic pH (pH 3–5), **6** displayed a significantly larger  $\alpha$ -helix content, which represents an opposite trend relative to the secondary structure changes of native albumin proteins<sup>16</sup> at low pH, again highlighting the unique structural characteristics of **6**. With increasing pH,  $\beta$ -sheet and random coil structural elements became more predominant. The larger content of structurally more rigid  $\alpha$ -helix elements at low pH likely imposes restrictions on the ability of the polymer backbone to conform to the surface of the QD and allow for more ligand–QD interactions. Additionally, we expect a decline in the number of thiol–QD binding interactions in accordance with previously observed dissociation of thiolate ligands from QDs at low pH,<sup>17</sup> leading to less surface passivation and low QYs. However, with increasing pH and in particular above pH 7, more  $\beta$ -sheet as well as flexible random coil structural elements occur, which can facilitate anchoring of more of the thiol and amine groups on the polymer backbone to the QD surface, thus leading to increased QYs. These dramatic changes of the secondary structure may thus play a significant role in the observed trends in pH responsiveness of the coated QDs **7**. The exact identities of the resultant trapped states formed or removed at different pH, appropriately probed with fast time-resolved techniques, was beyond the scope of this work and will be reported at a later time.

DLS and TEM were used to investigate the average diameter  $d$  of **7** in solution (Figure 4b) and on a surface (Figure 4a). It was found that the samples contained mostly single, isolated QDs. The average diameter of **7** was  $29.4 \pm 3.9$  nm with a narrow size distribution (Figure 4b). A few clusters were detected by TEM; they may have formed during the solvent evaporation process. The

*d* values of **7** at different pH were also investigated using DLS. Only a slight increase in *d* between pH 3 and 9 was detected. Therefore, the altered emission intensity is attributed to passivation events on the QD surface, and pH-induced aggregate formation is unlikely.

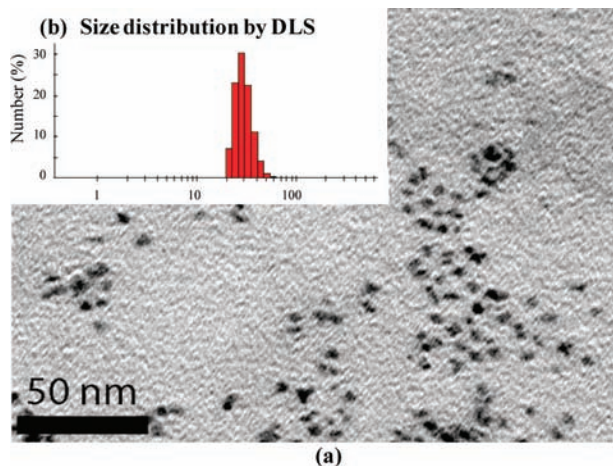


**Figure 4.** (a) TEM picture of **7**. (b) Typical size distribution for **7** according to DLS.

**Table 1.** Fluorescence Quantum Yields (QY), Total Emission Intensities (EI), and diameters (*d*) for **7** and Corresponding Conformational Changes of **6** at Different pH Values

pH	EI ± S.D.	QY ± S.D. (%)	conformations of <b>6</b>				<i>d</i> ± S.D. (nm) <sup>a</sup>
			α-helix (%)	β-turn (%)	β-sheet (%)	r. coil (%)	
3	0.40 ± 0.14	5.5 ± 1.7	70.7	12.6	1.2	1.6	23.5 ± 5.01
5	0.54 ± 0.11	12.3 ± 1.6	63.8	9.7	8.8	17.7	30.2 ± 3.13
7	0.94 ± 0.12	16.0 ± 0.9	36.8	5.2	26.5	31.6	29.4 ± 3.93
9	1.71 ± 0.31	23.2 ± 1.2	30.3	3.1	33.7	32.9	37.0 ± 7.56

<sup>a</sup> Average diameter recorded by DLS after a minimum of two independent measurements at different pH.

In summary, a facile approach toward multifunctional side-chain peptide–polymer hybrids based on a linear albumin backbone is presented for the first time. Such macromolecules possess unique features such as an accurately known length and a defined number of functional groups at distinct locations within the albumin peptide backbone, low size dispersity, and intrinsic biocompatibility. Multiple PEO and dithiotic acid anchor groups were introduced via an orthogonal functionalization strategy that allowed for

multivalent interactions with QDs and their subsequent stabilization in water. The resulting peptide–polymer-coated QDs displayed acceptable QYs of up to 26% and remained aggregation-free in aqueous solution for several months. Interestingly, a significant influence of the pH on the QY of the coated QDs was found, which was fully reversible at physiological pH. These changes were attributed to conformational rearrangements of the peptide backbone of the dHSA–PEO–TA hybrids **6**, which likely influenced the amount of surface passivation by the functional groups on the polymer brush moiety. Further development of these peptide–polymer-coated QDs into biocompatible pH sensors is currently ongoing.

**Acknowledgment.** This work was supported by NUS Startup Grants WBS-R143-000-393-646 and WBS-R143-000-367-133.

**Supporting Information Available:** Experimental details regarding the synthesis and characterization techniques used for structures **4**, **6**, and **7** and the core–shell CdSe–CdZnS QDs. This material is available free of charge via the Internet at <http://pubs.acs.org>.

## References

- (1) Michalet, X.; Pinaud, F. F.; Bentolila, L. A.; Tsay, J. M.; Doose, S.; Li, J. J.; Sundaresan, G.; Wu, A. M.; Gambhir, S. S.; Weiss, S. *Science* **2005**, *307*, 538.
- (2) Hezinger, A. F. E.; Tessmar, J.; Göferich, A. *Eur. J. Pharm. Biopharm.* **2008**, *68*, 138.
- (3) Liu, W.; Greytak, A. B.; Lee, J.; Wong, C. R.; Park, J.; Marshall, L. F.; Jiang, W.; Curtin, P. N.; Ting, A. Y.; Nocera, D. G.; Fukumura, D.; Jain, R. K.; Bawendi, M. G. *J. Am. Chem. Soc.* **2010**, *132*, 472.
- (4) Uyeda, H. T.; Medintz, I. L.; Jaiswal, J. K.; Simon, S. M.; Mattoussi, H. *J. Am. Chem. Soc.* **2005**, *127*, 3870.
- (5) Yu, M. W.; Chang, E.; Falkner, J. C.; Zhang, J.; Al-Somali, A. M.; Sayes, C. M.; Johns, J.; Drezek, R.; Colvin, V. L. *J. Am. Chem. Soc.* **2007**, *129*, 2871.
- (6) Susumu, K.; Uyeda, H. T.; Medintz, I. L.; Pons, T.; Delehanty, J. B.; Mattoussi, H. *J. Am. Chem. Soc.* **2007**, *129*, 13987.
- (7) Medintz, I. L.; Farrell, D.; Susumu, K.; Trammell, S. A.; Deschamps, J. R.; Brunel, F. M.; Dawson, P. E.; Mattoussi, H. *Anal. Chem.* **2009**, *81*, 4831.
- (8) Liu, W.; Howarth, M.; Greytak, A. B.; Zheng, Y.; Nocera, D. G.; Ting, A. Y.; Bawendi, M. G. *J. Am. Chem. Soc.* **2008**, *130*, 1274.
- (9) Susumu, K.; Mei, B. C.; Mattoussi, H. *Nat. Protoc.* **2009**, *4*, 424.
- (10) Suzuki, M.; Husimi, Y.; Komatsu, H.; Suzuki, K.; Douglas, K. T. *J. Am. Chem. Soc.* **2008**, *130*, 5720.
- (11) Snee, P. T.; Somers, R. C.; Nair, G.; Zimmer, J. P.; Bawendi, M. G.; Nocera, D. G. *J. Am. Chem. Soc.* **2006**, *128*, 13320.
- (12) Chen, Y.; Thakar, R.; Snee, P. T. *J. Am. Chem. Soc.* **2008**, *130*, 3744.
- (13) Algar, W. R.; Krull, U. J. *ChemPhysChem* **2007**, *8*, 561.
- (14) Liu, W.; Choi, H. S.; Zimmer, J. P.; Tanaka, E.; Frangioni, J. V.; Bawendi, M. G. *J. Am. Chem. Soc.* **2007**, *129*, 14530.
- (15) Jeong, S.; Achermann, M.; Nanda, J.; Ivanov, S.; Klimov, V. I.; Hollingsworth, J. A. *J. Am. Chem. Soc.* **2005**, *127*, 10126.
- (16) El Kadi, N.; Taulier, N.; Le Huérou, J. Y.; Gindre, M.; Urbach, W.; Nwigwe, I.; Kahn, P. C.; Waks, M. *Biophys. J.* **2006**, *91*, 3397.
- (17) Aldana, J.; Lavelle, N.; Wang, Y.; Peng, X. *J. Am. Chem. Soc.* **2005**, *127*, 2496.

JA909570V